NJC



PAPER

View Article Online
View Journal | View Issue



Cite this: *New J. Chem.*, 2014, **38**, 2394

# Synthesis, crystal structure, and optical characteristics of $[Pd_2Hg_4Cl_6\{Te(DMB)\}_6]\cdot 2DMF$, $[HgClTe(DMB)]_4$, and the ring-forming cluster $[Pd_{12}(TePh)_{24}]\cdot 2DMF$†

Barbara Tirloni,[a] Ernesto Schulz Lang,*[b] Gelson Manzoni de Oliveira,*[b] Paulo Piquini[c] and Manfredo Hörner[b]

Received (in Victoria, Australia) 21st November 2013,
Accepted 22nd January 2014

DOI: 10.1039/c3nj01455j

www.rsc.org/njc

The clusters here discussed represent improvements to our preparative techniques directed toward the synthesis of ternary nanoclusters of the type MM′Te. $Hg(TeR)_2$ (R = $(2,6\text{-}OCH_3)_2C_6H_3$) reacts with $PdCl_2$ to give $[Pd_2Hg_4Cl_6\{(TeR)\}_6]\cdot 2DMF$ (**1**) and $[HgClTeR]_4$ (**2**), and further with $Pd(O_2CCH_3)_2$ to give $[Pd_{12}(TePh)_{24}]\cdot 2DMF$ (**3**). The core of compound **1** was analysed by first principles DFT and the results confirm the existence of two systems 3c–4e$^-$, in which the two $Te^{II}$ atoms act as bridging ligands. While compound **2** appears to provide the driving force for the formation of cluster **1**. In the case of metallocycle **3**, the driving force guiding the reaction probably originates from the mercury salts ($HgCl_2$ or $Hg(Ac)_2$) formed during the process.

## Introduction

The chemistry of the heavier organochalcogen ligands toward group 10 transition metals constitutes a growing area of development in organometallic chemistry.[1] Interest in this area arises from the multidisciplinary applications of these complexes, which can serve as single-source precursors for binary transition metal selenides and tellurides in material science,[2] as well as homogeneous catalysts.[3] The oxidative addition of E–E bonds (E = S, Se, Te) to low-valence transition metal complexes is a basic process of organometallic chemistry and provides a mild and simple way to synthesize chalcogenolato complexes through the cleavage of the E–E bond. In some instances, however, the bond remains intact, as highlighted by Singh and co-workers.[4,5] On the other hand, the reaction of the ditellurides with M(0) (M = Ni, Pd, Pt) could result in the cleavage of a C–E bond.[6]

The Hg–ER clusters (E = Se, Te; R = aryl) and the oxidative additions of halogenides to E–E bonds (E = Se, Te) represent our main results hitherto;[7,8] however, these studies also bore implications for the development of efficient strategies for creating large molecular architectures that display certain desired properties, including catalysis, hydrogen release, or biomimetic synthetic models of natural systems. The development of strategies for preparing large functional architectures is one of the most important goals in modern supramolecular chemistry.

Very few clusters containing Te and Pd form Te–Pd bonds or interactions. When present, these interactions are complex and unusual, similar to the complexities observed by Singh[4] in the context of the oxidative addition of E–E bonds to low-valence transition metal complexes. For example, the cluster $[Pd_3(\mu_3\text{-}Te)_2(DPPP)_3]Cl_2\cdot 3CHCl_3$ (DPPP = 1,3-bis(diphenylphosphino)-propane), reported by Kedarnath *et al.*,[9] forms two atypical triple bridges involving two telluride ions ($Te^{2-}$), both linked to three $Pd^{II}$ centers. The same authors showed, in $[PdCl\{2\text{-}Te(Cl)_2C_5H_3(3\text{-}Me)N\}(PPh_3)]$, that the assignment of formal oxidation numbers {$Te^{IV}$ and $Pd^{II}$} can be a complicated task. Gabbaï and Lin[10] isolated a Te–Pt complex having a covalent Te–Pt bond polarized toward the platinum atom, which led the authors to speculate that telluronium ions may behave as σ-acceptors (or Z ligands) to form transition metal complexes. A Z-type ligand refers to a ligand that accepts two electrons from the metal center.[11] The authors[10] showed that telluronium cations could behave as Z-ligands toward transition metals. Additionally, the cations displayed the propensity to act as Lewis acid ligands toward transition metals, similar to other high-valence fifth period species.

[a] *Faculdade de Ciências Exatas e Tecnologia, Universidade Federal da Grande Dourados, 79804-970, Dourados, MS, Brazil. E-mail: batirloni@yahoo.com.br*
[b] *Departamento de Química, Universidade Federal de Santa Maria, UFSM, 97105900, Santa Maria, RS, Brazil. E-mail: eslang@smail.ufsm.br, manzonideo@smail.ufsm.br, hoerner.manfredo@gmail.com; Fax: +55 55-3220-8031*
[c] *Departamento de Física, Universidade Federal de Santa Maria, UFSM, 97105900, Santa Maria, RS, Brazil. E-mail: ppiquini@gmail.com*

† Electronic supplementary information (ESI) available: Crystallographic parameters and details of data collection and refinement; graphical determination of the $E_g$ value of **1** and **2**; Fig. S1–S4. CCDC 947899 (**1**), 947900 (**2**) and 947901 (**3**). For ESI and crystallographic data in CIF or other electronic format see DOI: 10.1039/c3nj01455j

 

The tetravalent telluronium$^{III}$ cations in the unusual complexes reported receive one electron pair from a pentavalent $Pd^{IV}$ center. The same authors obtained a $Te^{III}$–$Pt^{III}$ complex with a covalent Te–Pt bond.[12] Platinum and tellurium complexes that deviated from the common telluroether–metal and telurolate–metal chemistry were reported. These complexes included uncommon (X-ray characterized) $Te^{0}$–$Pt^{II}$ bonds.[13] The cluster complexes described herein are consistent with recent trends in modern chemistry toward understanding the interactions between tellurium and transition metals. With the aim of expanding our research into the preparation of ternary architecturally large MM′E nanoclusters, we report the synthesis, structural characterization, and optical properties of the new clusters $[Pd_2Hg_4Cl_6\{Te(DMB)\}_6]\cdot 2DMF$ (**1**) (DMB = 2,6-dimethoxybenzene; DMF = dimethylformamide), $[HgClTe(DMB)]_4$ (**2**), and the ring-forming nanocluster $[Pd_{12}(TePh)_{24}]\cdot 2DMF$ (Ph = phenyl) (**3**).

## Discussion

The reaction steps involved in the preparation of the compounds reported in this work are summarized in Chart 1. Clusters **1**, **2** and **3** were obtained from $Hg(TeR)_2$ (R = DMB and Ph) and palladium salts, since $Hg(TeR)_2$ compounds display a reactivity similar to that of a Grignard reagent, while enabling control over the structural growth of the products. The growth of complexes **1** and **3** was controlled by the steric effects of the substituents DMB (**1**) and phenyl groups (**3**) bonded to the tellurium atoms. Compound **2** can be considered as one of the secondary products generated in these reactions.

The molecular structure of the cluster **1** is shown in Fig. 1.

The structure and chemical composition of $[Pd_2Hg_4Cl_6\{Te(DMB)\}_6]\cdot 2DMF$ (**1**) are novel, and no other combination of the atoms Pd, Hg, Te, and Cl has been reported previously. The molecular structure of **1** was achieved by linking two moieties of $\{PdHg_2[Te(2,6\text{-}OCH_3)_2C_6H_3]_2Cl_3\}$ to form a centrosymmetric unit. Each molecule was accompanied by two solvating DMF molecules in the crystal lattice. Complex **1** is a {HgTePd} ternary compound bearing a core formed by four Hg atoms, two Pd, and six Te atoms. In this structure, the metallic centers are connected through $[\mu\text{-}Te(2,6\text{-}OCH_3)_2C_6H_3]^-$ groups. The primary coordination geometry around the Pd center is a distorted parallelogram; however, the coordination sphere includes two additional long range interactions: Pd1···Cl2 (3.4994(22)) and Pd1···O2 (2.8514(51) Å). These extra interactions induce a distorted octahedral coordination geometry around the Pd center. The primary trigonal coordination around Hg1 is distorted to form a tetrahedral geometry through the Hg1···O3 interaction (2.665(2) Å). The trigonal coordination around the Hg2 center becomes trigonal bipyramidal due to the presence of the Hg1···O3 bond (2.665(2) Å) and a Hg–π interaction (Hg2···$\eta^6$-π-aryl, 3.3856(4) Å) with the aromatic $(2,6\text{-}OCH_3)_2C_6H_3$ ring. The Hg–π distance agrees with the value reported in the literature.[14] The secondary interactions represented by "···" reach distances that are longer than the sum of the covalent radii and shorter than the sum of the van der Waals radii of the respective elements. The sums of the van der Waals radii are 3.60 (Hg/O), 3.85 (Pd/Cl), and 3.60 Å (Pd/O).[15] The bonds Pd1′–Te1′–Pd1 and Pd1′–Te1–Pd1 represent two systems 3c–4e$^-$ in which the two $Te^{II}$ atoms act as bridging ligands. The Te1–Te1′ interaction, with a distance of 3.2851(6) Å, is predominantly covalent because the van der Waals radius of Te is 2.06 Å and the Te–Te bond distance of the *M*-enantiomer of the simplest diaryl ditelluride PhTe–TePh is 2.7073(5) Å.[16] The Te1–Te1′ interaction was expected to weaken the Te–Pd bonds within the 3c–4e$^-$ system by decreasing the electron density on the tellurium atoms and lowering the Te–Pd bond orders. The Te–Pd bonds inside the 3c–4e$^-$ system measure 2.5945(7) and 2.5699(8) Å, whereas the Te–Pd bonds outside the ring are 2.6143(8) and 2.6209(7) Å in length. The Te–Te and Te–Pd bond orders in the 3c–4e$^-$ system and the extent to which the Te–Te interaction lowers the Te–Pd bond orders were investigated by conducting first-principles DFT calculations. The natural bond order analysis allows us to study the inner structure of cluster **1** and the central core formed by Te1, Te1′, Pd1, Pd1′, in particular. The Wiberg[17] bond indices determined from the self-consistent-field calculations

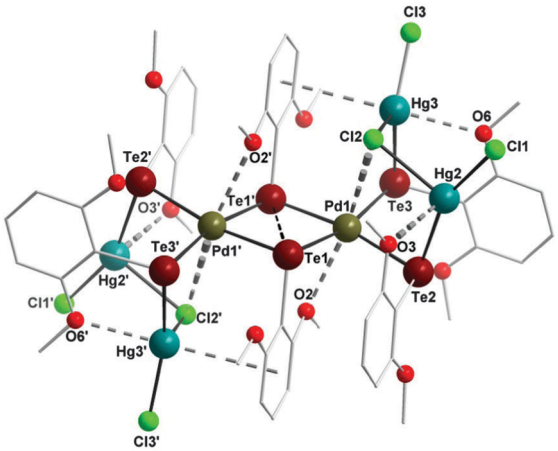


Fig. 1 Structure of $[Pd_2Hg_4Cl_6\{Te(DMB)\}_6]\cdot 2DMF$ (**1**). For clarity, the hydrogen atoms and the solvent molecules (DMF) are not shown. Symmetry transformations used to generate equivalent atoms: (′) $-x+1, -y+1, -z+1$. Selected bond lengths [Å] and angles [°]: Hg1–Cl1 2.355(2), Hg1–Cl2 2.690(3), Hg1–Te2 2.7034(7), Hg1–O3 2.665(2), Hg2–O6 2.676(64), Hg2–Cl2 2.665(2), Hg2–Cl3 2.365(2), Hg2–Te3 2.6423(6), Pd1–Te1 2.5700(7), Pd1′–Te1 2.5945(8), Pd1–Te2 2.6210(8), Pd1–Te3 2.6142(7), Pd1···Cl2 3.4994(22), Pd1–O2 2.85514(51); Te1–Pd1–Te1′ 79.00(2), Te1–Pd1–Te3 166.31(3), Te1′–Pd1–Te3 90.67(2), Te1–Pd1–Te2 97.30(2), Te1′–Pd1–Te2 169.59(3), Te3–Pd1–Te2 94.36(2), Cl1–Hg1–Te2 156.98(9), Cl1–Hg1–Cl2 96.04(10), Te2–Hg1–Cl2 106.91(5), Cl3–Hg2–Te3 154.91(8), Cl3–Hg2–Cl2 97.08(9), Te3–Hg2–Cl2 107.36(5), C1–Te1–Pd1 101.4(2), C1–Te1–Pd1′ 98.4(2), Pd1–Te1–Pd1′ 101.00(2).

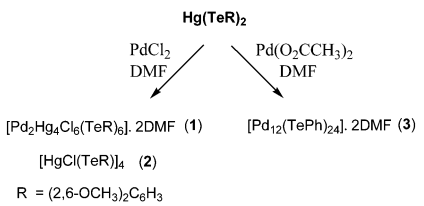


Chart 1 Reactions involved in the preparation of the compounds reported in this work.

Table 1 Calculated Wiberg bond indices for bonds involving the Te atoms

| Atomic pair | Te1–Te1′ | Te1–Pd1 | Te1–C | Te2–Pd1 | Te2–Hg1 | Te2–C |
|---|---|---|---|---|---|---|
| Wiberg bond index | 0.28 | 0.55 | 0.88 | 0.49 | 0.66 | 0.88 |

suggested a classical example of bond multiplicity. The calculated Wiberg indices are shown in Table 1 for some of the bonds involving Te atoms. The values reported in Table 1 suggest a Wiberg index of 0.28 for the Te1–Te1′ bond. The presence of this weak Te1–Te1′ bond reduces the Te1–Pd1 (Te1–Pd1′, Te1′–Pd1 and Te1′–Pd1′) bond order, which was found to be 0.55, by decreasing the electron density on the Te1 and Te1′ atoms. Although the Te2–Pd1 bond order is smaller than the bond order of Te1–Pd1, the calculated positive charge on Te1 (0.61) is almost twice the value calculated for Te2 (0.33), indicating that the Te1–Te1′ bond significantly reduces the electron density on the Te1 and Te1′ atoms.

These results support the 3c–4e$^-$ model of the Pd1′–Te1′–Pd1 and Pd1′–Te1–Pd1 bonds, in which the Te1 and Te1′ centers act as bridging ligands. The natural bond order analysis revealed the presence of two bonding (and two anti-bonding) 'bridging' Te1–Te1′ orbitals, as partially shown in Fig. 2. The 'bridging' bonding orbital with the lowest eigenvalue is sp in character and is oriented along the line joining the Te1 and Te1′ atoms (Fig. 2a). The other bonding orbital involving the Te bridging atoms is π-like in character and includes p-orbitals from Te1 and Te1′ along the lines joining the Te and Pd atoms, as shown in Fig. 2b. The corresponding anti-bonding orbitals are shown in the ESI.†

Another alternative for the 3c–4e$^-$ model for the core of compound **1** would be the treatment of the Pd atoms as central $Pd^{2+}$ ones in the $d^8$ configuration with a $dsp^2$ hybrid in the classical Pauling's VB model and square planar coordination with four 2c–2e$^-$ bonds, just as in a classical complex. The first principles DFT calculations, as well as the distorted octahedral coordination of the two palladium atoms, however, give support to the 3-centered bond model.

The molecular structure of compound **2**, $[HgClTe(dmb)]_4$, is formed by two asymmetric units. The cluster relies on the formation of an 8-membered ring with alternating Te and Hg atoms. Compound **2** appears to provide the driving force for the formation of cluster **1**. The centrosymmetric molecular structure of **2** was prepared by the interactions of two groups $Hg\{Te(2,6\text{-}OCH_3)_2C_6H_3\}_2$ stabilized by two Cl$^-$ ligands, which were further connected to two moieties of {HgCl} through the tellurium atoms of the $Hg\{Te(2,6\text{-}OCH_3)_2C_6H_3\}_2$ groups.

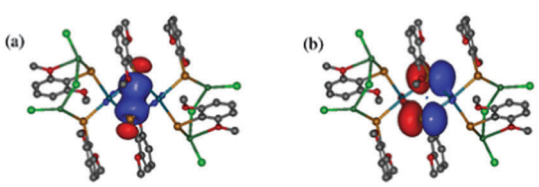


Fig. 2 Natural bond orbitals between Te1 and Te1′ atoms in the central ring. (a) An sp-like bonding orbital. (b) A π-like bonding orbital.

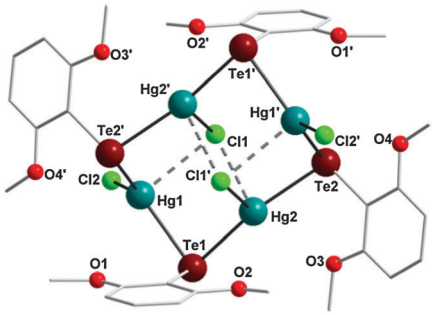


Fig. 3 Structure of $[HgClTe(DMB)]_4$ (**2**). For clarity, the hydrogen atoms are not shown. Symmetry transformations used to generate equivalent atoms: (′) $-x, -y + 2, -z + 1$. Selected bond distances [Å] and angles [°]: Hg1–Cl1 2.9652(9), Hg1–Cl2 2.4281(10), Hg1–Te1 2.7682(3), Hg1–Te2′ 2.7525(3), Hg1′–Te2 2.7525(3), Hg2–Cl1 2.9601(9), Hg2–Cl1′ 2.7280(8), Hg2′–Cl1 2.7280(8), Hg2–Te1 2.6874(3), Hg2–Te2 2.6938(3); Cl2–Hg1–Te2′ 122.06(3), Cl2–Hg1–Te1 118.48(3), Te2′–Hg1–Te1 118.100(8), Cl2–Hg1–Cl1 97.83(3), Te2′–Hg1–Cl1 89.781(17), Te1–Hg1–Cl1 94.011(18), Te1–Hg2–Te2 159.756(9), Te1–Hg2–Cl1′ 103.90(2), Te2–Hg2–Cl1′ 96.28(2), Te1–Hg2–Cl1 95.840(19), Te2–Hg2–Cl1 83.055(19), Cl1′–Hg2–Cl1 88.24(2), Hg2–Te1–Hg1 85.441(7), Hg2–Te2–Hg1′ 89.129(8).

The primary coordination geometry around the Hg atoms is trigonal planar, and this geometry becomes tetrahedral in the presence of the intramolecular Hg···Cl interactions. The Hg1 atom forms covalent bonds with Te1, Te2′, and Cl2 and a secondary interaction with Cl1. The Hg2 atom forms covalent bonds with Te1, Te2 and Cl1′, and a secondary interaction with Cl1. The Hg1···Cl1/Hg1′···Cl1′ secondary interactions span a distance of 2.9652(9) Å, whereas the Hg2···Cl1/Hg2′···Cl1′ secondary bonds are 2.9601(9) Å. The lengths of these Hg–Cl interactions exceed the sum of the Hg–Cl covalent radii but are shorter than the sum of the van der Waals radii for Hg and Cl, 3.85 Å.[15] The molecular structure of cluster **2** is illustrated in Fig. 3.

The optical band gap of the compounds **1** and **2** could be estimated based on the UV-Vis diffuse reflectance spectra. The material absorption coefficient ($\alpha$) of a layer with infinite thickness can be related to the sample diffuse reflectance ($r$) by the Kubelka–Munk function (1):[18]

$$\left(\frac{\alpha}{s}\right) = \frac{(1-r)^2}{2r} \quad (1)$$

where $s$ is the material scattering coefficient. Experimentally, this expression can be applied to powdered samples because the layer formed by a powder is continuous and behaves as an infinite medium.[18] Furthermore, light scattering can be assumed to be wavelength-independent for particles greater than 5 μm in size.[19] The compound layer fulfilled these requirements, so it was possible to estimate the optical band gap energy ($E_g$) based on the sample absorption spectrum calculated from relation (1).[20] The plots of $(\alpha/s)^2$ (ref. 20) *versus* energy for the compounds displayed a steep absorption edge. The $E_g$ value was obtained for **1** and **2** by extrapolating the steep absorption edge to the crossing with the energy axis (see ESI†).[20] As a result, the values of 1.94 and 2.04 eV were obtained for the band gaps of **1** and **2**.

 

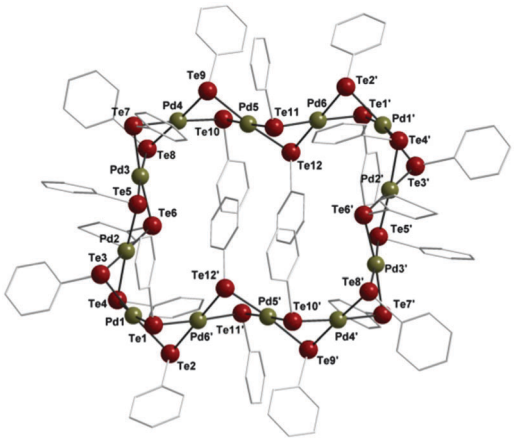


Fig. 4 Molecular structure of the macrocyclic compound $[Pd_{12}(TePh)_{24}]\cdot 2DMF$ (**3**). For clarity, the hydrogen atoms and the solvent molecules (DMF) are not shown. Symmetry transformations used to generate equivalent atoms: (′) $-x + 0.5, -y + 0.5, -z + 1$. Selected bond lengths [Å] and angles [°]: Pd1–Te1 2.5909(16), Pd1–Te2 2.6085(16), Pd1–Te3 2.5908(16), Pd1–Te4 2.5965(16), Pd6–Te1′ 2.5906(14), Pd6–Te2′ 2.6014(15), Pd6–Te11 2.5993(14), Pd6–Te12 2.5847(15), Pd1–Pd6′ 3.1872(17); Te3–Pd1–Te1 94.76(5), Te3–Pd1–Te4 83.23(5), Te1–Pd1–Te4 172.29(6), Te3–Pd1–Te2 174.78(6), Te1–Pd1–Te2 83.43(5), Te4–Pd1–Te2 97.92(5), Te12–Pd6–Te1′ 94.66(5), Te12–Pd6–Te11 84.88(4), Te1′–Pd6–Te11 177.27(6), Te12–Pd6–Te2′ 177.76(5), Te1′–Pd6–Te2′ 83.58(4), Te11–Pd6–Te2′ 96.95(5), Pd6′–Te1–Pd1 75.92(4), Pd6′–Te2–Pd1 75.43(4).

Organochalcogenolates of $Pd^{II}$ and $Pt^{II}$ are versatile molecular precursors of the metal chalcogenides, an important family of functional inorganic materials with applications in electronic and optoelectronic devices.[21] The square planar geometry of a Pd center allows the formation of polymeric systems or geometric self-assembled structures in the form of giant squares (metallocycles), as demonstrated by Lee and Lin.[22] The molecular structure of the new macrocyclic nanocluster $[Pd_{12}(TePh)_{24}]\cdot 2DMF$ (**3**) is illustrated in Fig. 4. The macrocycle **3** comprises two asymmetric units. Each molecular formula includes two solvent DMF molecules. The 12 Pd atoms in the macrocyclic ring form a distorted square planar coordination geometry and are linked by 24 anionic bridges of the type $[\mu\text{-TePh}]^-$. The nanocluster **3** is centrosymmetric, and the Pd–Te bond distances are in the range 2.5847(15)–2.6085(16) Å. The greatest intramolecular distance between the Pd atoms is 14.8114(17) Å. The greatest intramolecular distance between tellurium atoms is 15.1312(17) Å.

The band gap of the macrocyclic nanocluster **3** could not be estimated using diffuse reflectance spectroscopy because an adequate diffuse reflectance spectrum could not be obtained. The dark black crystals did not reflect radiation in the UV-Vis band. After some measurement attempts, the crystals were found to be markedly decomposed.

## Conclusions

The structures of $[Pd_2Hg_4Cl_6\{Te(DMB)\}_6]\cdot 2DMF$ (**1**) $[HgClTe(DMB)]_4$ (**2**) and $[Pd_{12}(TePh)_{24}]\cdot 2DMF$ (**3**) were characterized and DFT calculations were performed to elucidate the nature of the bonds in the central ring of cluster **1**, revealing that the Te–Te bond coexists with the Te–Pd bonds in 3c–4e$^-$ systems. This structure represents an example of the many possible chemical intermediates formed during organometallic chemistry reactions. The band gaps of clusters **1** and **2** were determined (1.94 and 2.04 eV, respectively), based on optical spectroscopy measurements. A suitable diffuse reflectance spectrum of the nanocluster **3** could not be acquired in the UV-Vis range (and the band gap could not be measured). The results reported in this paper suggest that mercury derivative chemical intermediates can pave the way for the syntheses of compounds with a high structural complexity. The methods developed here provide a gentle and simple approach to the syntheses of chalcogenolate complexes, such as compound **3**. The tellurium–metal, telluroethers–metal, and telurolate–metal interactions were characterized and revealed uncommon Te–metal bonds.[4–6,9–13] This intermediate structure permits the use of synthetic routes that involve mild methodologies, while also enabling a high level of control over the desired products.

## Experimental section

All syntheses were conducted under an Ar atmosphere. The compounds $Hg(TePh)_2$ and $Hg\{Te(DMB)\}_2$ were prepared according to procedures reported in the literature.[23,24] All other analytical grade reagents and solvents were obtained commercially (Aldrich or Vetec), and the solvents were freshly distilled prior to use. FTIR spectra were recorded on a BRUKER FTIR model Tensor 27 spectrophotometer over the range 4000–400 $cm^{-1}$. Elemental analyses (CHN) were determined using a VARIO EL (Elementar Analysen systeme GmbH)).

### Preparations and tools

**1. Preparation of $[Pd_2Hg_4Cl_6\{Te(DMB)\}_6]\cdot 2DMF$ (1).** To a solution of 0.097 g (0.133 mmol) $Hg\{Te(2,6\text{-}OCH_3)_2C_6H_3\}_2$ in 5 mL DMF was added 0.018 g (0.1 mmol) $PdCl_2$. The color of the mixture turned from a greenish yellow to a dark red. The solution was stirred for 4 h at room temperature and filtered through Celite. Red crystals of the product were obtained by lowering the temperature of the mother solution. Yield: 0.026 g, 27% based on $Hg\{Te(2,6\text{-}OCH_3)_2C_6H_3\}_2$. *Properties*: air stable, red crystalline substance. Calcd for $C_{54}H_{68}Cl_6Hg_4N_2O_{14}Pd_2Te_6$ (2962.56): C, 21.89; H, 2.29%. Found: C, 20.09; H, 1.86%. IR (KBr): 3052 [$\nu_s$(C–H)$_{Ar}$]; 2933 [$\nu_{as}$(C–H)$_{Me}$]; 2831 [$\nu_s$(C–H)$_{Me}$]; 1672 [$\nu$(C═O)]; 1578, 1463, 1426 [$\nu_s$(C═C)]; 1242 [$\nu_{as}$(C–O–C)]; 1098 [$\nu_s$(C–O–C)]; 763, 738 [$\delta_{op}$(C═C–H)]; 607 $cm^{-1}$ [$\delta_{op}$(C═C–C)]. (Ar = aromatic; Me = methyl; $\delta_{ip}$ = deformation in the plane; $\delta_{op}$ = deformation out of the plane).

**2. Preparation of $[HgClTe(DMB)]_4$ (2).** To a solution of 0.073 g (0.1 mmol) $Hg\{Te(2,6\text{-}OCH_3)_2C_6H_3\}_2$ in 5 mL DMF was added 0.018 g (0.1 mmol) $PdCl_2$. The mixture turned from a greenish yellow to a dark brown. After 1 h of stirring at room temperature, the solution was filtered through Celite. A layer of 5 mL isopropanol was carefully spread across the interface of the mother solution, which yielded monocrystals suitable for X-ray diffractometric analysis. Yield: 0.009 g, 18% based on $Hg\{Te(2,6\text{-}OCH_3)_2C_6H_3\}_2$. *Properties*: air stable, dark brown

crystalline substance. Calcd for $C_{32}H_{36}Cl_4Hg_4O_8Te_4$ (2003.17): C, 19.19; H, 1.81%. Found: C, 19.43; H, 1,77%. IR (KBr): 3051 [$\nu_s$(C–H)$_{Ar}$]; 2939 [$\nu_{as}$(C–H)$_{Me}$]; 2833 [$\nu_s$(C–H)$_{Me}$]; 1582, 1466, 1427 [$\nu$(C=C)]; 1248 [$\nu_{as}$(C–O–C)]; 1101 [$\nu_s$(C–O–C)]; 772, 738 [$\delta_{op}$(C=C–H)]; 594 $cm^{-1}$ [$\delta_{op}$(C=C–C)].

**3. Preparation of $[Pd_{12}(TePh)_{24}]\cdot 2DMF$ (3).** To a suspension of 0.061 g (0.1 mmol) $Hg(TePh)_2$ in 5 mL DMF was added 0.022 g (0.1 mmol) of $Pd(O_2CCH_3)_2$. The mixture turned from an orange to a dark brown color, and a dark brown precipitate formed. After 2 h of stirring at room temperature, the mixture was filtered. After dissolving the precipitate in pyridine, dark brown crystals of **3** were obtained from the filtrate. Yield: 0.021 g, 41% based on $Hg(TePh)_2$. *Properties*: air stable, black crystalline substance. Calcd for $C_{150}H_{134}N_2O_2Pd_{12}Te_{24}$ (6335.80): C, 28.43; H, 2.13; N, 0.44%. Found: C, 28.07; H, 1.95; N, 0.53%.

**4. X-Ray diffraction.** A Bruker CCD X8 APEX II diffractometer was used for the X-ray structure analyses. The equipment was operated using a graphite monochromator with Mo-K$\alpha$ radiation ($\lambda$ = 0.71073 Å). The structure was refined using a full-matrix least squares on $F^2$ using all data (SHELX crystal structure solution software). The structure was solved with SHELXS using direct methods.[25] All non-hydrogen atoms were refined using anisotropic displacement parameters in SHELXL.[25] The hydrogen atom positions were calculated starting from the idealized positions. The free refinement of hydrogen atom parameters gave a low data/parameter ratio and led to high correlations. Details about the structure determination steps are provided in the ESI.†

**5. Computational methodology.** Density functional theory calculations were performed to analyze the bonding properties of cluster **1**. The hybrid B3LYP functional[26] was used to describe the exchange and correlation term of the effective Kohn–Sham potential. The Pople 6-31G basis set augmented with d and p polarization functions was used to model the light atoms (H, C, O, Cl).[27] The basis set used to model the heavy atoms (Pd, Te, Hg) was the Stevens/Basch/Krauss split valence CEP-31G.[28] The geometry of cluster **1**, as extracted from the X-ray diffraction data, was optimized based on an analysis of the vibrational frequencies. The resultant configuration was (at least) a local minimum. All calculations were performed using the Gaussian 09 code.[29] Plots of the natural orbitals were prepared using the GabEdit software.[30]

**6. Diffuse reflectance spectroscopy.** The optical band gap characterization of compounds **1** and **2** was possible by using a CARY 5000 spectrometer outfitted with a diffuse reflectance accessory to measure the diffuse reflectance spectra over the UV-Vis wavelength range (200–800 nm). The compounds were studied in a powdered form that included very large particles. The particles were characterized by forming a layer of the analyzed sample material over a glass slab. A baseline was acquired using the light intensity reflected by a PTFE standard plate, $R_{Std}$. The detector noise signal, $R_{Noise}$, was also characterized. No sample was placed in the reflectance diffuse accessory during the acquisition of the baseline and detector noise signals. The light intensity reflected by the sample ($R_{Sample}$) was then measured, and the sample diffuse reflectance was calculated according to the ratio $r = (R_{Sample}/(R_{Std} - R_{Noise})$ (see ESI†).

## Notes and references

1 (*a*) A. K. Singh and S. Sharma, *Coord. Chem. Rev.*, 2000, **209**, 49; (*b*) W. Levason, S. D. Orchard and G. Reid, *Coord. Chem. Rev.*, 2002, **225**, 159; (*c*) V. K. Jain, L Jain, *Coord. Chem. Rev.*, 2005, **249**, 3075; (*d*) M. N. Sokolova and P. A. Abramova, *Coord. Chem. Rev.*, 2012, **256**, 1972.

2 (*a*) M. A. Malik, P. O'Brien and N. Revaprasadu, *Phosphorus, Sulfur Silicon Relat. Elem.*, 2005, **180**, 689; (*b*) A. Kornienko, S. Banerjee, G. A. Kumar, R. E. Riman, T. E. Emge and J. G. Brennan, *J. Am. Chem. Soc.*, 2005, **127**, 14008; (*c*) H. Zhang, D. Wang and H. Möhwald, *Angew. Chem., Int. Ed.*, 2006, **45**, 748; (*d*) L. B. Kumbhare, V. K. Jain, P. Phadnis and M. Nethaji, *J. Organomet. Chem.*, 2007, **692**, 1546 and references therein.

3 (*a*) G. Zeni, A. L. Braga and H. A. Stefani, *Acc. Chem. Res.*, 2003, **36**, 731; (*b*) G. Zeni, D. S. Ludtke, R. B. Panatieri and A. L. Braga, *Chem. Rev.*, 2006, **106**, 1032; (*c*) B. C. Ranu, K. Chattopadhyay and S. Banerjee, *J. Org. Chem.*, 2006, **71**, 423.

4 T. Chakrabortya, K. Srivastava, H. B. Singh and R. J. Butcher, *J. Organomet. Chem.*, 2011, **696**, 2782.

5 (*a*) H. Matsuzaka, T. Ogino, M. Nishio, M. Hidai, Y. Nishibayashi and S. Uemura, *J. Chem. Soc., Chem. Commun.*, 1994, 223; (*b*) H. B. Singh, A. Regini, J. P. Jasinsky, E. S. Paight and R. J. Butcher, *J. Organomet. Chem.*, 1994, **466**, 283; (*c*) W. Baratta and P. S. Pregosin, *Inorg. Chem.*, 1994, **33**, 4494.

6 (*a*) L. B. Han, N. Choi and M. Tanaka, *J. Am. Chem. Soc.*, 1997, **119**, 1795; (*b*) L. B. Han, S. Shimada and M. Tanaka, *J. Am. Chem. Soc.*, 1997, **119**, 8133; (*c*) L. B. Han and M. Tanaka, *Chem. Commun.*, 1998, 47; (*d*) A. Khanna, B. L. Khandelwal, A. K. Saxena and T. P. Singh, *Polyhedron*, 1995, **14**, 2705.

7 (*a*) G. A. Casagrande, E. S. Lang, G. M. Oliveira, M. Hörner and F. Broch, *Inorg. Chim. Acta*, 2007, **360**, 1776; (*b*) E. S. Lang, B. Tirloni, G. M. Oliveira and M. A. Villetti, *Inorg. Chim. Acta*, 2009, **362**, 3114; (*c*) E. S. Lang, G. M. Oliveira, B. Tirloni and M. A. Villetti, *J. Cluster Sci.*, 2008, **19**, 459; (*d*) E. S. Lang, G. M. Oliveira, B. Tirloni, A. B. Lago and E. M. Vázquez-López, *J. Cluster Sci.*, 2009, **20**, 467; (*e*) B. Tirloni, E. S. Lang and G. M. Oliveira, *Polyhedron*, 2013, **62**, 126.

8 (*a*) G. M. Oliveira, E. Faoro and E. S. Lang, *Inorg. Chem.*, 2009, **48**, 4607; (*b*) E. Faoro, G. M. Oliveira and E. S. Lang, *J. Organomet. Chem.*, 2009, **694**, 1557; (*c*) E. Faoro, G. M. Oliveira and E. S. Lang, *Polyhedron*, 2009, **28**, 63; (*d*) E. Faoro, G. M. Oliveira, E. S. Lang and C. B. Pereira, *J. Organomet. Chem.*, 2011, **696**, 807.

9 R. S. Chauhan, G. Kedarnath, A. Wadawale, A. M. Z. Slawin and V. K. Jain, *Dalton Trans.*, 2013, **42**, 259.

10 T. P. Lin and F. P. Gabbaï, *Angew. Chem., Int. Ed.*, 2013, **52**, 3864.

 

11 M. L. H. Green, *J. Organomet. Chem.*, 1995, **500**, 127.
12 T. P. Lin and F. P. Gabbaï, *J. Am. Chem. Soc.*, 2012, **134**, 12230.
13 R. S. Chauhan, G. Kedarnath, A. Wadawale, A. Muñoz-Castro, R. Arratia-Perez, V. K. Jain and W. Kaim, *Inorg. Chem.*, 2010, **49**, 4179.
14 I. A. Tikhonova, D. A. Gribanyov, K. I. Tugashov, F. M. Dolgushin, A. S. Peregudov, D. Y. Antonov, V. I. Rosenberg and V. B. Shur, *J. Organomet. Chem.*, 2010, **695**, 1949.
15 A. Bondi, *J. Phys. Chem.*, 1964, **68**, 441.
16 (*a*) A. L. Fuller, L. A. S. Scott-Hayward, Y. Li, M. Bühl, A. M. Z. Slawin and J. D. Woollins, *J. Am. Chem. Soc.*, 2010, **132**, 5799; (*b*) G. Llabres, O. Dideberg and L. Dupont, *Acta Crystallogr., Sect. B: Struct. Crystallogr. Cryst. Chem.*, 1972, **28**, 2438.
17 K. B. Wiberg, *Tetrahedron*, 1968, **24**, 1083.
18 W. W. M. Wendlant and H. G. Hecht, *Reflectance Spectroscopy – Chemical Analysis 21*, Interscience Publishers (John Wiley & Sons), New York, 1966, pp. 113–114.
19 O. Reckeweg, C. Lind, A. Simon and F. J. Z. DiSalvo, *Z. Naturforsch.*, 2003, **58B**, 159.
20 V. Derstroff, J. Ensling, V. Ksenofontov, P. Gütlich and W. Z. Tremel, *Z. Anorg. Allg. Chem.*, 2002, **628**, 1346.
21 V. K. Jain, L. B. Kumbhare, S. Dey and N. D. Ghavale, *Phosphorus, Sulfur Silicon Relat. Elem.*, 2008, **183**, 1003.
22 S. J. Lee and W. Lin, *Acc. Chem. Res.*, 2008, **41**, 521.
23 N. Petragnani, *Tellurium in Organic Synthesis*, Academic Press, London, 1994.
24 M. Bochmann and K. J. Webb, *J. Chem. Soc., Dalton Trans.*, 1991, 2325.
25 G. M. Sheldrick, *Acta Crystallogr., Sect. A: Found. Crystallogr.*, 2008, **64**, 112.
26 (*a*) A. D. Becke, *J. Chem. Phys.*, 1993, **98**, 5648; (*b*) C. Lee, W. Yang and R. G. Parr, *Phys. Rev. B: Condens. Matter Mater. Phys.*, 1988, **37**, 785.
27 W. J. Hehre, R. Ditchfield and J. A. Pople, *J. Chem. Phys.*, 1972, **56**, 2257.
28 W. J. Stevens, M. Krauss, H. Basch and P. G. Jasien, *Can. J. Chem.*, 1992, **70**, 612.
29 M. J. Frisch, G. W. Trucks, H. B. Schlegel, G. E. Scuseria, M. A. Robb, J. R. Cheeseman, G. Scalmani, V. Barone, B. Mennucci, G. A. Petersson, H. Nakatsuji, M. Caricato, X. Li, H. P. Hratchian, A. F. Izmaylov, J. Bloino, G. Zheng, J. L. Sonnenberg, M. Hada, M. Ehara, K. Toyota, R. Fukuda, J. Hasegawa, M. Ishida, T. Nakajima, Y. Honda, O. Kitao, H. Nakai, T. Vreven, J. A. Montgomery Jr., J. E. Peralta, F. Ogliaro, M. Bearpark, J. J. Heyd, E. Brothers, K. N. Kudin, V. N. Staroverov, R. Kobayashi, J. Normand, K. Raghavachari, A. Rendell, J. C. Burant, S. S. Iyengar, J. Tomasi, M. Cossi, N. Rega, N. J. Millam, M. Klene, J. E. Knox, J. B. Cross, V. Bakken, C. Adamo, J. Jaramillo, R. Gomperts, R. E. Stratmann, O. Yazyev, A. J. Austin, R. Cammi, C. Pomelli, J. W. Ochterski, R. L. Martin, K. Morokuma, V. G. Zakrzewski, G. A. Voth, P. Salvador, J. J. Dannenberg, S. Dapprich, A. D. Daniels, Ö. Farkas, J. B. Foresman, J. V. Ortiz, J. Cioslowski and D. J. Fox, *Gaussian 09, Revision C.01*, Gaussian, Inc., Wallingford CT, 2009.
30 A. R. Allouche, *J. Comput. Chem.*, 2011, **32**, 174.